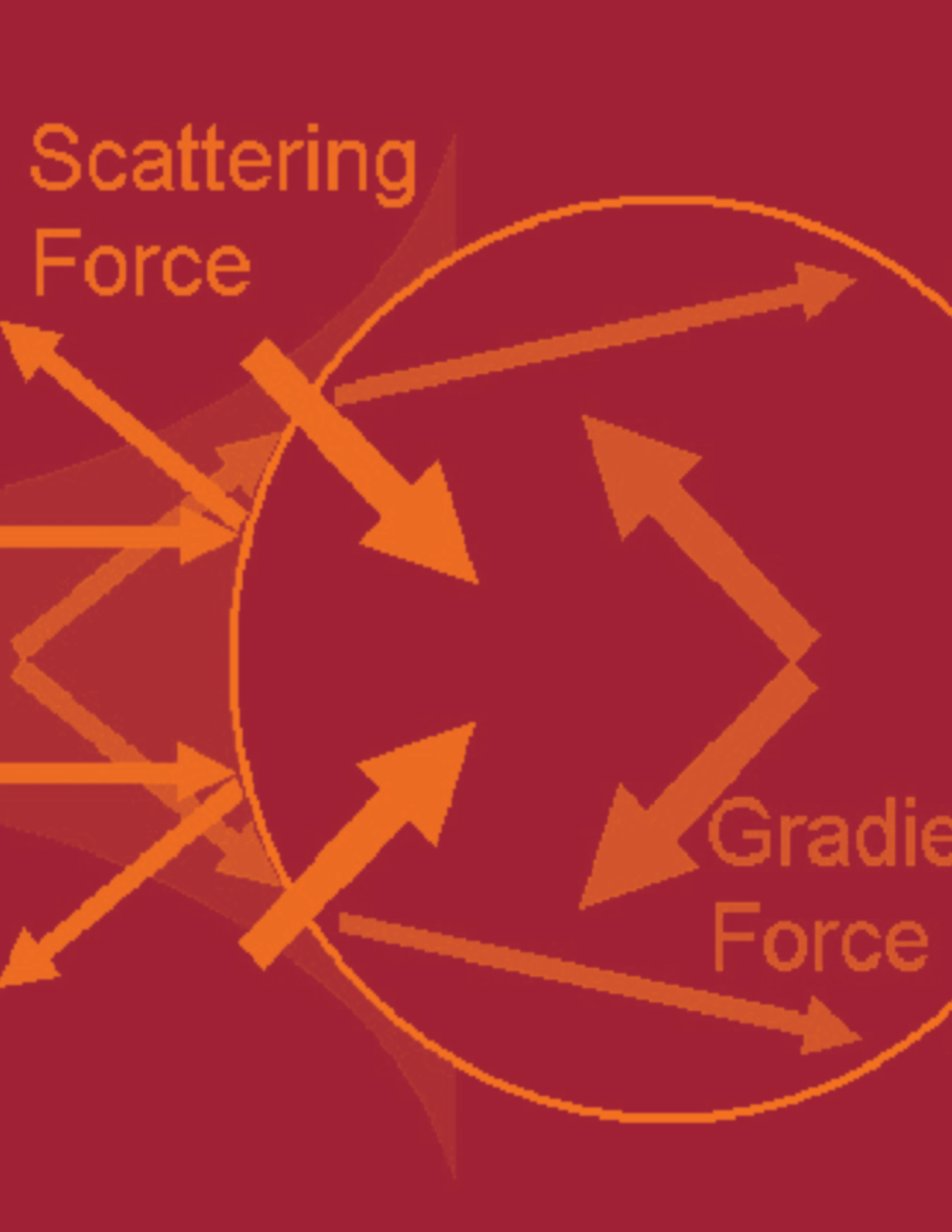
Scattering
Force
Gradie
Force

Optical Particle Sorting in Translating Brownian Liquids

Undergraduate Researcher
Paul West
Michigan Technological University

Faculty Mentor
John B. Ketterson
Department of Physics and Astronomy and of Electrical Engineering and Computer Science
Northwestern University

Graduate Student Mentor
Weiqiang Mu
Department of Physics and Astronomy
Northwestern University

Abstract

In this research project, particle sorting of Brownian liquids was explored by sweeping two noncoherent pairs of parallel optical standing waves in a translating medium. Each wave was created by interfering two coherent beams of light, and the resulting fringe periods were determined by the angle of intersection. Adjusting the fringe spacing of wave ridges allows application of an optical force to particles of one size while minimizing or nullifying the force on particles of another size. Exploiting this method is potentially the foundation for a noninvasive cell and virus sorting technique. The random nature of Brownian motion on these particles was also explored.

Introduction

Optical tweezing and particle sorting have proven to be powerful tools in the fields of physics and biology. Applications of these techniques include, but are not limited to, the sorting and manipulation of cancer and reproductive cells, as well as viruses and bacteria.[1] Similar techniques can be used to study the physical properties of DNA and RNA, and can be extended to nanometer-sized particles — including those smaller than the wavelength of light.[2] Conventional methods of particle manipulation often require physical contact with the sample. Laser tweezing surmounts these traditional methods because the force applied to the sample is exclusively optical.

Background

The technique of laser tweezing was first explored in 1970[3,4] as a way of trapping and manipulating micron-sized particles using only light from a single laser beam. This beam was tightly focused onto a sample, which created an optical force (roughly in the range of piconewtons to femtonewtons) on micron-sized particles. The optical force arises from a combination of scattering and a gradient in the intensity (Figure 1). Soon after the technique of optical tweezing was discovered, it was utilized for particle sorting.[5,6] Various techniques have been established over the past several years,[7–19] and two groups have recently reported approaches for sorting different-sized particles using a translating optical standing wave.[15,16,27] The lateral force on a particle from a standing wave is determined by the wave spacing relative to the particle diameter. Adjusting these parameters allows particles to sort by size. Particles of one size will "slip" from one standing wave intensity maximum to an adjacent trailing one because of a very small force acting upon them, while particles of another size will move along with the wave as it is translated. In addition, the particles are subjected to Brownian motion — a physical phenomenon observed with microscopic particles immersed in a liquid that causes them to move about randomly.

Approach

As discussed above, an optical standing wave has the ability to trap particles of one size while leaving behind particles of another size. A Matlab® computer simulation was written to model how particles behave in Brownian liquids under two nominally standing optical waves that are translated in opposite directions. The standing wave spacing, speed of translation, number of particles, laser intensity, and time duration of the simulation are the inputs for the computer model. The output is a diagram showing how the particles' sizes compare with average speed of translation.

In this experiment, a Spectra Physics Millenia laser (532 nm) with a full power of 4 W operating in TEM00 mode was used. The laser output first travels through an adjustable telescope that allows for changing the diameter of the laser beam. The telescope was tuned to increase the Gaussian waist (the narrowest part of a focused laser beam) such that it occupied a larger area. This improves the chance of the sample particles moving with the standing wave instead of collecting in the region of the maximum of the beam intensity. The

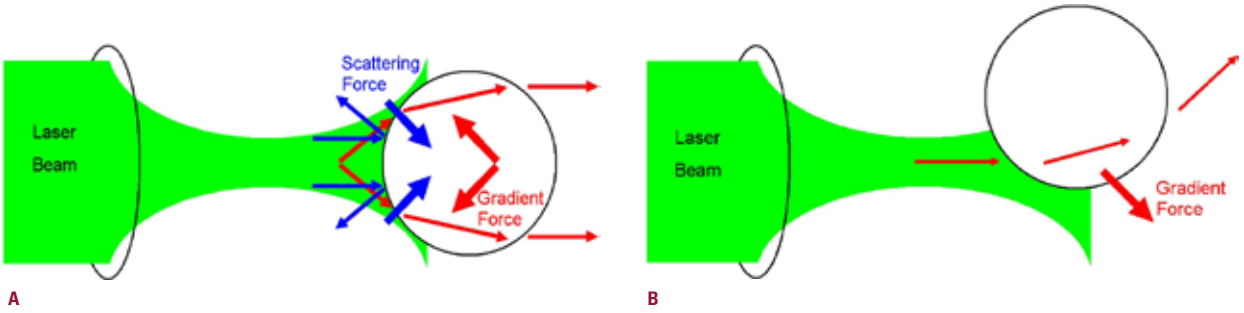

Figure 1. Diagram illustrating the gradient and scattering forces on a particle caused by the change in momentum of the light. Figure (A) illustrates a particle in equilibrium. Figure (B) illustrates the gradient force pulling the particle towards the center of the beam.

beam is then split with three nonpolarizing beam splitters into four beams of equal intensity (Figure 2).

These two noncoherent pairs of beams are independently reflected off adjustable prism mirrors. The beams are then focused with an objective lens, causing the beams to overlap one another at the Gaussian waist associated with the geometrical focal point. The pairs of overlapping coherent (waves of the same phase) beams interfere with one another, creating a standing wave. The distance (d) between standing wave ridges is $d_n = \lambda / (2\sin(\theta_n / 2))$, where n represents a pair of coherent beams, λ is the wavelength of the laser beam (532 nm), and θ_n is the angle between the pair of converging beams. The adjustable mirrors can be used to individually vary the spacing between beams, thereby changing θ, which in turn adjusts the distance between standing wave nodes.

In this experiment, 2-and 3-µm-diameter polystyrene spheres were used. Figure 3 shows that the diminishing force for the 2- and 3-µm particles occurs when the standing wave distance is 1.43 and 1.94 µm, respectively. By adjusting the mirrors, wave ridges d_1 and d_2 were set to their corresponding spacings. This yields a condition where wave 1 produces a force on particle 1 while vanishing for particle 2 in the absence of wave 2; correspondingly, wave 2 produces a force on particle 2 while vanishing for particle 1 in the absence of wave 1. The experiment and the simulations explore the behavior when both beams are present. In addition, the sample stage is mounted on a motor-driven translator, allowing the particles to be continually sorted by moving the sample perpendicular to the direction of the translating standing waves.

The polystyrene spheres used in these experiments were monodispersed to more than 4% and diluted in deionized water. A hole was punched in double-sided Scotch Tape™ (~80 µm thick), and the sample was sealed inside this tape between two No. 2 microscope cover glasses (Fisherbrand 12-540A 18X18), preventing capillary or evaporative flows. In principle, a variety of samples can be used for this experiment, including silica, bacteria, viruses, and human cells; however, the sample must have a greater refractive index than its surrounding medium. Polystyrene samples are used because organic samples would be destroyed by the intense heat generated via optical absorption from the laser beam. Using an infrared laser can minimize this problem. However, such lasers are both inconvenient and dangerous; because the output is not in the visible spectrum, one has to be careful to avoid inadvertent skin and eye contact.

The sample is placed at the focal point of the objective lens, and the optical standing waves created are observed through the microscope; small particles are attracted to the standing wave intensity maxima. The optical interference patterns are translated by applying voltages to a pair of piezoelectric displacers, which shift the optical phase of one beam relative to the other. This causes the interference patterns to move horizontally, parallel to the cover slips but in opposite directions; the motor-driven translator continuously displaces the sample vertically.

Results

The computer simulations provide interesting results. For example, particles have a greater tendency to become trapped in slower-moving standing waves

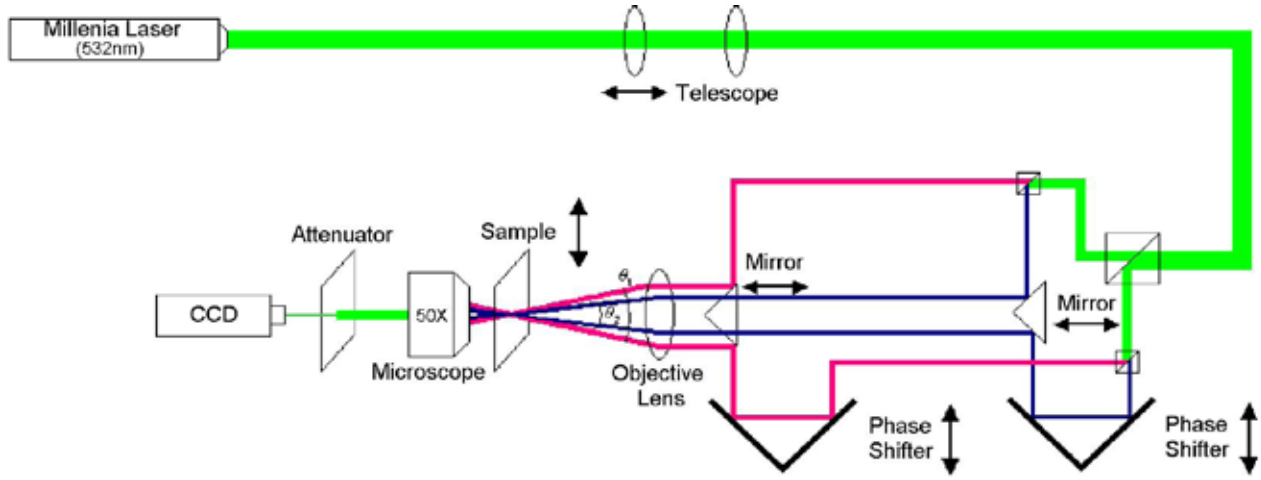

Figure 2. Schematic of the interferometery set-up. Pink and blue beams are colored for convenience only. The phase-shifting mirrors are mounted on piezoelectric displacers, which in turn are mounted on an optical translator. The sample has the ability to be moved perpendicular to the direction of the translating standing waves.

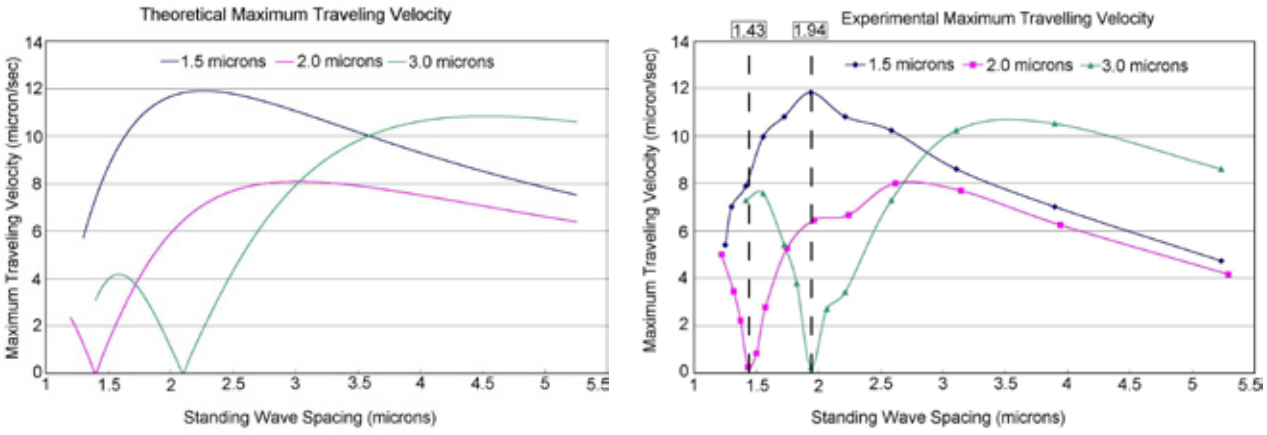

A **B**

Figure 3. Graphical representation of the (A) theoretical and (B) experimental values for the maximum displacement velocity for differently sized particles. The theoretical curves show the absolute value obtained from the Rayleigh scattering theory. The dashed lines in (B) represent standing wave spacings corresponding to a vanishing optical force on the particle (where it always slips). These standing wave spacings are the basis of the optical sorting process.

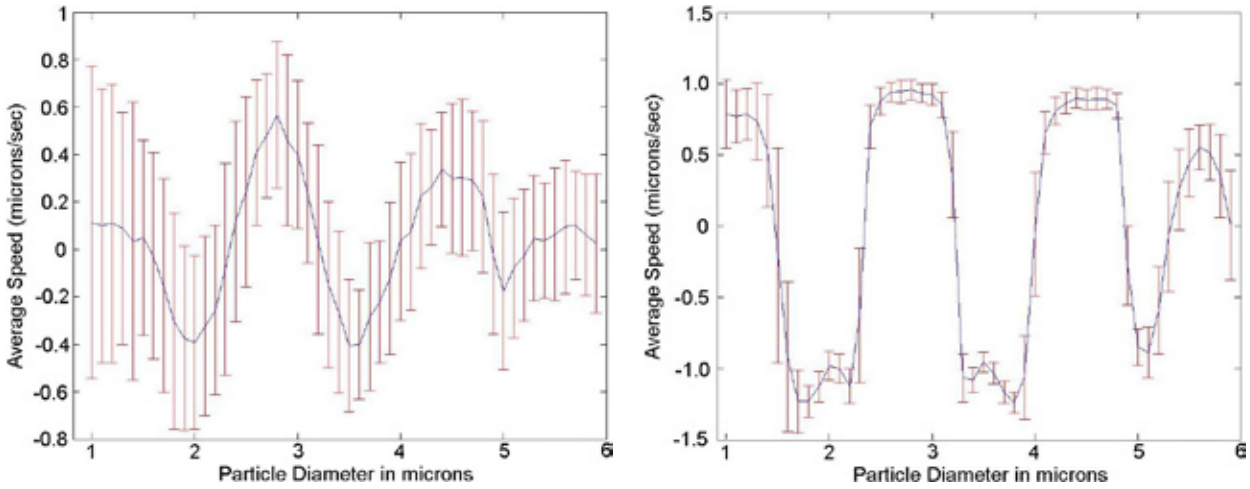

Figure 4. Output from computer simulation showing in figure (A) a relatively weak optical force (0.01 pN) and (B) a relatively strong optical force (0.05 pN). The standing wave speed in both simulations was 1 µm/sec in both directions. Blue lines represent average speeds. Red "bars" represent one standard deviation.

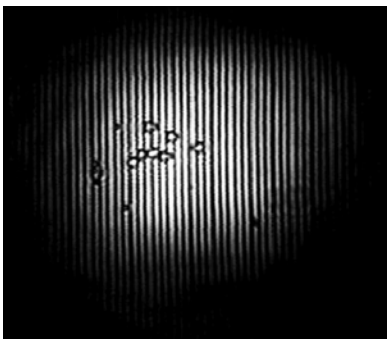

Figure 5. Image of the optical standing wave. Particles can be seen "trapped" on the white lines, which are the standing wave intensity maxima.

because the optical force is greater than the viscous drag. Another interesting result is shown in Figure 4 from two simulations involving translations at 1 µm/sec in each direction with different laser intensities. When the standing wave periods are correctly adjusted and translated at 1 µm/sec in both directions, the 2-µm particles will move to the left and 3 µm particles will move to the right. When the optical force is only 0.01 pN, the 2- and 3-µm particles move on average 0.4 µm/sec, with a standard deviation of about 0.7 µm/sec, illustrating poor trapping (not traveling with the wave). However, when the intensity is increased to 0.05 pN and translated at the same speed, the 2- and 3-µm particles both move at an average speed of about 1 µm/sec, with a standard deviation of only 0.3 µm/sec. These graphs demonstrate that when the laser intensity increases, not only do the particles tend to move with the standing wave in opposite directions, but also their standard deviations dramatically reduce. This demonstrates that when particles are strongly "trapped" on their respective standing wave maxima, they are much less likely to "slip" or "jump" from one intensity maximum to another.

When a sample was prepared containing both 2- and 3-µm particles mixed randomly in the solution, and the adjustable mirrors were calibrated to create standing waves with spacings of 1.43 and 1.94 µm, particles of both sizes tended to be attracted toward the center of the Gaussian beam where the optical intensity is largest (Figure 5). Applying a voltage to the piezoelectric displacers caused the standing waves to be displaced in opposite horizontal directions, pulling the corresponding particles along – 2 µm to the left and 3 µm to the right. The sample was then translated vertically to

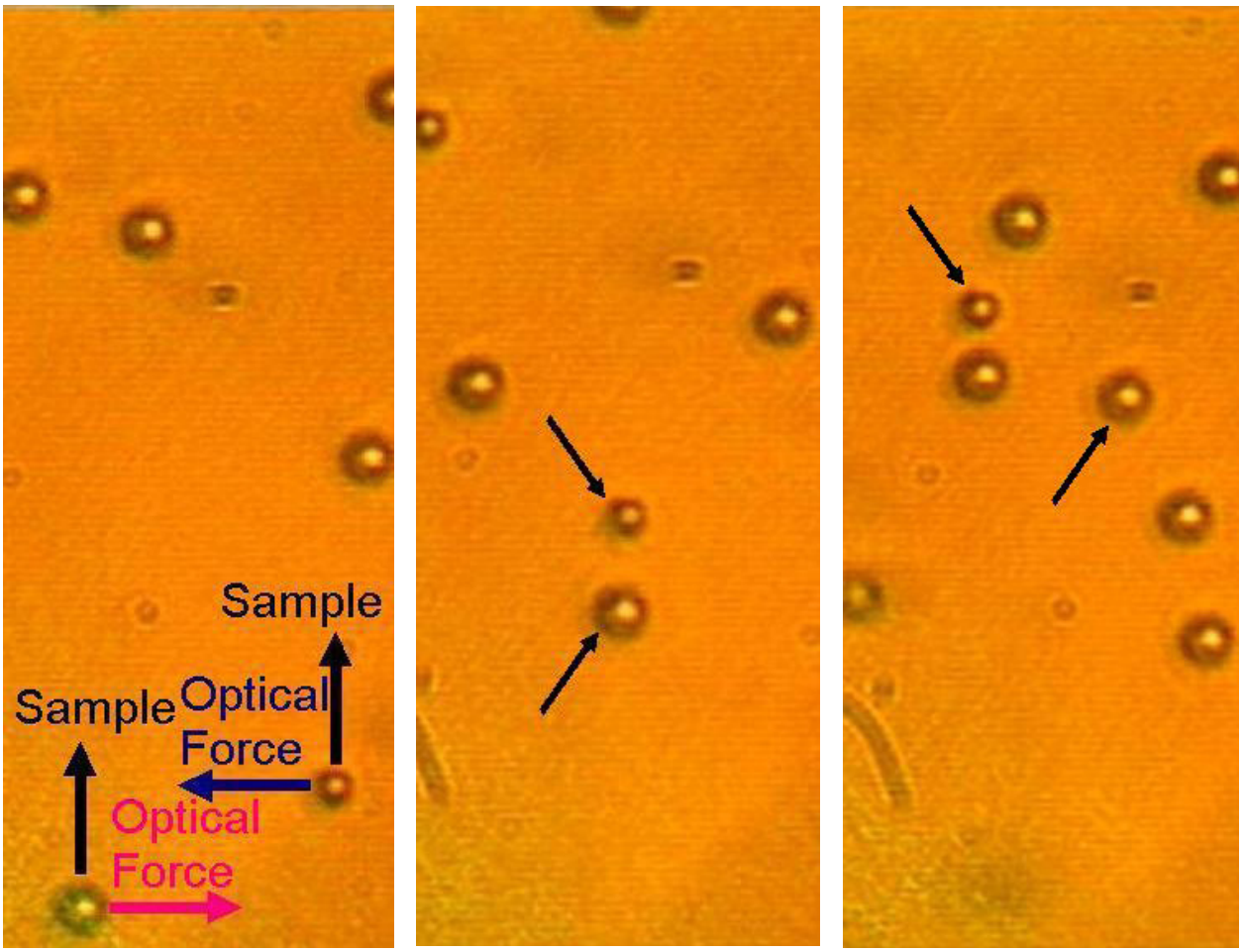

Figure 6. Series of photographs taken approximately 2 sec apart. (A) shows the vectors (not to scale) of the optical force and direction of sample movement. The circles in (B) and (C) are shown to identify the original particles (blue for the 2 µm, pink for 3 µm).

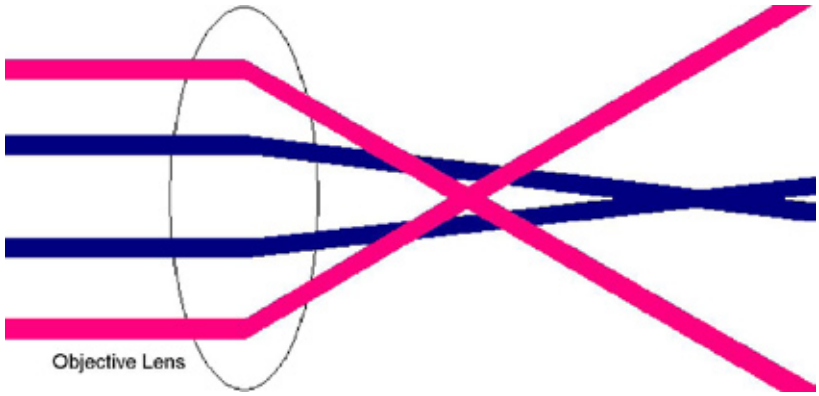

Figure 7. Illustration exaggerating the spherical aberration phenomena. As light moves from the outside of the lens to the inside, the focal point of these beams moves farther from the lens.

separate particles throughout — a more efficient optical sorting technique. This procedure is shown in Figure 6.

Discussion

The beam size on the sample is extremely critical. The force on the particles is linear to the laser intensity, which diminishes with the inverse square of the beam radius ($W/\pi r^2$). When the beam waist is too small, the intensity in the center of the beam will cause the particles to "slip" from one standing wave maxima to another — thereby staying in the center of the Gaussian beam rather than translating with the wave. Another drawback of a tightly focused beam is that the gradient force on the particles is greater than the viscous drag when the sample is vertically translated. This will also cause the particles to have a tendency to be trapped in the center of the beam. When the beam size on the sample is too large, the viscous and Brownian forces surmount the optical force.

Focusing two differently-spaced parallel beams of light may result in spherical aberration. A pictorial representation of this phenomenon is shown in Figure 7. The closer the beams are to the center of the lens, the further from the lens they will focus. This can be problematic because it is impossible to focus parallel beams on the same point using a spherical lens. An ideal solution to this problem is to use an aspherical lens. However, because the two focal points were separated by less than 1 µm, spherical aberration had negligible effects on the results.

The computer simulation demonstrates that different-sized particles can be pulled in opposite directions under correct conditions. However, the simulation does not take into account the Gaussian distribution of the laser intensity. While the results are reasonably accurate for particles near the center of the beam, their validity diminishes as the distance from this point increases.

Conclusion

The research described provides interesting experimental and theoretical behaviors related to optical displacement and sorting in translating Brownian particle systems. Research in this laboratory, using similar techniques, has already begun to sort different-sized biological cells, vesicles, etc., with an infrared laser. Of particular interest may be stretching or squeezing cells (or arrays of cells) using standing waves. Polystyrene beads can be bonded to DNA, allowing the molecule to be manipulated (e.g., stretched) with the laser to study its physical properties. Experiments in the lab have already begun using three and four coherent laser beams to create differently-shaped optical standing wave interference patterns. While conventional methods of biological particle sorting and manipulation require physical contact, the techniques of laser tweezing are noninvasive, allowing one to use samples that would otherwise be destroyed or damaged by traditional methods.

This research was supported primarily by the Nanoscale Science and Engineering Initiative of the National Science Foundation under NSF Award Number ***EEC-0647560.*** *Any opinions, findings and conclusions or recommendations expressed in this material are those of the author(s) and do not necessarily reflect those of the National Science Foundation.*

References

(1) Grover, S. C.; Skirtach, A. G.; Gauthier, R. C. *J. Biomed. Opt.* **2001,** *6.*

(2) Wang, M. D.; Yin, H.; Landick, R. *Biophys. J.* **1997,** *72* (3), 1335–1346.

(3) Ashkin, A. *Phys. Rev. Lett.* **1970,** *24,* 156.

(4) Ashkin, A; Dzidezic, J. M.; Bjorkholm, J. E.; Chu, S. *Opt. Lett.* **1986,** *11,* 288.

(5) Buican, T; Smyth, M. J.; Crissman, H. A.; Salzman, G. C.; Stewart, C. C.; Martin, J. C. *Appl. Opt.* **1987,** *26,* 5311.

(6) Imasaka, T.; Kawabata, Y.; Kaneta, T.; Ishldzu, Y. *Anal. Chem.* **1995,** *67,* 1763.

(7) Macdonald, M. P.; Spalding, G. C.; Dholakia, K. *Nature* **2003,** *426,* 421.

(8) Ladavac, K.; Kasza, K.; Grier, D. G. *Phys. Rev. E.* **2004,** *70,* 010901.

(9) Hart, S. J.; Terray, A. V. *Appl. Phys. Lett.* **2003,** *83,* 5316.

(10) Wang, M. M.; Tu, E.; Raymond, E. E.; et al. *Nat. Biotechnol.* **2005,** *23,* 83.

(11) Grujic, K.; Helleso, O. G.; Hole, J. P.; Wilkinson, J. S. *Opt. Express.* **2004,** *13,* 5747.

(12) Xie, C.; Chen, D.; Li, Y. *Opt. Lett.* **2005,** *30,* 1800.

(13) Paterson, L.; Papagiakoumou, E.; Milne, G.; Garces-Chavez, V.; Tatarkova, S. A.; Sibbett, W.; Gunn-Moore, F. J.; Bryant, P. E.; Riches, A. C.; Dholakia, K. *Appl. Phys. Lett.* **2005,** *87* 123901.

(14) Applegate Jr., R. W.; Squier, J.; Vestad, T.; Oakey, J.; Marr, D. W. M. *Opt. Express* **2004,** *12,* 4390.

(15) Cizmar, T.; Siler, M.; Sery, M.; Zemanek, P.; Garces-Chavez, V.; Dholakia, K. *Phys. Rev.* **2006,** B74, *3*, 035105.

(16) Ricardez-Vargas, I.; Rodriguez-Montero, P.; Garcia-Romas, R.; Volke-Sepulveda, K. *Appl. Phys. Lett.* **2006,** *88,* 121116.

(17) Garces-Chavez, V.; Roskey, D.; Summers, M. D.; Melville, H.; Mcgloin, D.; Wright, E. M.; Dholakia, K. *Appl. Phys. Lett.* **2004,** *85,* 4001.

(18) Cheong, F. C.; Sow, C. H.; Wee, A. T. S.; Shao, P.; Bettiol, A. A.; VanKan, J. A.; Watt, F. *Appl. Phys. B – Lasers 0.* **2006,** *83,* 121.

(19) Rodrigo, P. J.; Eriksen, R. L.; Daria, V. R.; Gluckstad, J. *Opt. Express* **2002,** *10,* 1550.

(20) Broeck, C. V. D. *Europhys. Lett.* **1999,** *46,* 1.

(21) Chio, A. E.; Wang, W.; Soneck, G. J.; Hong, J.; Berns, M. W. *Opt. Commun.* **1997,** *133,* 7.

(22) Rubinov, A. N.; Katarkevich, V. M.; Afanas'ev, A. A.; Efendiev, T. Sh. *Op.t Commun.* **2003,** *224,* 97.

(23) Casaburi, A.; Pesce, G.; Zemanek, P.; Sasso, A. *Opt Commun.* **2005,** *251,* 393.

(24) Afanas'ev, A. A.; Rubinov, A. N.; Kurochkin, Y. A.; Mikhnevich, S. Y. U.; Ermolaev, I. E. *Quantum Electron.* **2003,** *33,* 250.

(25) Jezek, J.; Zemanek, P.; Jonas, A.; Sery, M; Pokorny, P.; Liska, M. *Proc SPIE Conf.* **2001,** 4356.

(26) Rohrback, A. and Sterzer, E. H. K. J. *Opt. Soc. Am. A* **2001,** *18,* 839.

(27) Mu, W.; Wang, G.; Spalding, G. C.; Luan, L.; West, P.; Kyriazes, H.; Ketterson, J. B., *Proc. SPIE Conf.* **2006,** 6326.